



Since January 2020 Elsevier has created a COVID-19 resource centre with free information in English and Mandarin on the novel coronavirus COVID-19. The COVID-19 resource centre is hosted on Elsevier Connect, the company's public news and information website.

Elsevier hereby grants permission to make all its COVID-19-related research that is available on the COVID-19 resource centre - including this research content - immediately available in PubMed Central and other publicly funded repositories, such as the WHO COVID database with rights for unrestricted research re-use and analyses in any form or by any means with acknowledgement of the original source. These permissions are granted for free by Elsevier for as long as the COVID-19 resource centre remains active.



Identification of novel transmembrane Protease Serine Type 2 drug candidates for COVID-19 using computational studies

Fatima A. Elbadwi^{a,1}, Elaf A. Khairy^{a,1}, Fatima O. Alsamani^{a,1}, Mariam A. Mahadi^{a,1},
Segood E. Abdalrahman^{a,1}, Zain Alsharf M. Ahmed^{a,1}, Inas Elsayed^b, Walaa Ibraheem^a,
Abdulrahim A. Alzain, PhD^{a,*}

^a Department of Pharmaceutical Chemistry, Faculty of Pharmacy, University of Gezira, Gezira, Sudan

^b Department of Pharmacology, Faculty of Pharmacy, University of Gezira, Gezira, Sudan

ARTICLE INFO

Keywords:

COVID-19
TMPRSS2
Drug repurposing
Homology modeling
Docking
Molecular dynamics

ABSTRACT

Severe acute respiratory syndrome coronavirus-2 (SARS-CoV-2) emergence has resulted in a global health crisis. As a consequence, discovering an effective therapy that saves lives and slows the spread of the pandemic is a global concern currently. *In silico* drug repurposing is highly regarded as a precise computational method for obtaining fast and reliable results. Transmembrane serine-type 2 (TMPRSS2) is a SARS CoV-2 enzyme that is essential for viral fusion with the host cell. Inhibition of TMPRSS2 may block or lessen the severity of SARS-CoV-2 infection. In this study, we aimed to perform an *in silico* drug repurposing to identify drugs that can effectively inhibit SARS-CoV-2 TMPRSS2. As there is no 3D structure of TMPRSS2 available, homology modeling was performed to build the 3D structure of human TMPRSS2. 3848 world-approved drugs were screened against the target. Based on docking scores and visual outcomes, the best-fit drugs were chosen. Molecular dynamics (MD) and density functional theory (DFT) studies were also conducted. Five potential drugs (Amikacin, isepamicin, butikacin, lividomycin, paromomycin) exhibited promising binding affinities. In conclusion, these findings empower repurposing these agents.

1. Introduction

A new severe acute respiratory syndrome coronavirus-2 (SARS-CoV-2) epidemic has started in Wuhan, China, in December 2019 [1]. Ever since, the epidemic has brought about 186.638 M confirmed cases and over 4 M deaths and inflicted considerable losses on the overall economy owing to city lockdowns [2–4]. Coronaviruses infect both animals and humans, causing a variety of ailments [5]. The three contagious viral human coronaviruses (hCoVs) that have been identified so far are MERS coronavirus, SARS coronavirus, and the 2019 coronavirus, which originated in Wuhan in December 2019 [6].

The pathogen is an RNA virus from the Coronavirinae subfamily in the Coronaviridae family of the order Nidovirales [7]. Spike, Membrane, Envelope, and Nucleocapsid proteins are the four main structural proteins encoded by the virus. S1 subunit promotes viral attachment to host cell surfaces. While, merging of membranes of viruses and cells, is carried out by the S2 subunit [8].

It is of great concern to find agents that can act early at the stage of the virus entry to the cell, ideally either inhibiting entry or diminishing the virus load that drives it into the cell [9].

The interaction of the virus with the host influences the occurrence and course of COVID-19 sickness [10]. The entry receptor for SARS-S is angiotensin-converting enzyme 2 (ACE2), while transmembrane Protease Serine Type 2 (TMPRSS2) is responsible for merging the viral and cellular membranes via the cleavage of S protein at the S1/S2 site. Thus the pathogenicity and virus dissemination is mainly due to the action of TMPRSS2 [11,12]. TMPRSS2 is expressed in all possible targets of SARS-CoV infection including; the prostate, cardiac endothelium, kidney, and digestive tract, suggesting that these organs may be important targets for SARS-CoV2 infection [4,13,14]. Therefore, the Inhibition of TMPRSS2 may block or lessen the severity of SARS-CoV-2 infections and its spreading [15,16].

However, development of novel drugs is a long process as it must go through extensive preclinical and clinical safety trials [9]. Hence,

* Corresponding author. 21111 Barakat Street, Medani, Gezira, Sudan.

E-mail addresses: awh3134@hotmail.com, abdulrahim.altoam@uofg.edu.sd (A.A. Alzain).

¹ Authors contributed equally.

<https://doi.org/10.1016/j.imu.2021.100725>

Received 2 August 2021; Received in revised form 1 September 2021; Accepted 3 September 2021

Available online 7 September 2021

2352-9148/© 2021 The Authors.

Published by Elsevier Ltd.

This is an open access article under the CC BY-NC-ND license

(<http://creativecommons.org/licenses/by-nc-nd/4.0/>).

repurposing of licensed drugs to prevent or limit SARS-COV2 viral propagation is now receiving interest for being cost-effective and time-saving, which is appropriate for the epidemic emergency [17].

Great efforts have been done to identify new treatments for COVID-19 [18–20]. Computer-assisted drug development (CADD) such as structure-based drug development is a widely utilized method for drug discovery [21]. CADD methods are becoming increasingly important in drug discovery, and they are vital in identifying viable therapeutic candidates at a low cost. These computational methods can help medicinal chemists and pharmacologists in the drug discovery process by minimizing the use of animal models in pharmaceutical investigation, assisting in the logical development of unique and safe medication candidates, repositioning marketed drugs, as well as assisting in the drug discovery process [22,23].

Many researchers utilized drug repurposing to combat COVID-19 [24]. It is worth mentioning that repurposing drugs have been less expensive in terms of both time and money. Because the majority of preclinical and clinical trials, including pharmacokinetic and toxicological studies of licensed or in clinical investigation phase's drugs, have already been reviewed, it takes less time to adapt them to a different indication. Toxicity and ADME (absorption, delivery, metabolism, and excretion) trials, which take a lot of time to finish, are not needed because the molecules under consideration for drug repositioning have indeed passed through these phases and have well-defined profiles. As a result, they are more appropriate for use in epidemics than novel molecules which have never been evaluated [25].

TMPRSS2 could be a promising target to develop agents to combat this crisis [17]. As far as we know, TMPRSS2 does not have tertiary structure [26]. Accordingly, our work aimed to: build a TMPRSS2 model, and then perform drug repurposing to discover novel inhibitors against TMPRSS2, which is an important target for SARS-CoV-2 entry into the host cell.

2. Methods

2.1. Homology modeling

As no crystal structure for TMPRSS2 is currently available in the PDB database, homology modeling was applied to build the protein model. The amino acid sequence of TMPRSS2 protein was retrieved in FASTA format from the UniProtKB database (Accession Number: O15393). BLASTp was used to identify human plasma kallikrein as the best template for homology modeling based on sequence similarity with sequence identity of 42.21% and sequence similarity of 47%. Accordingly, human plasma kallikrein 3D structure (PDB ID: 5TJX) [27] was obtained from protein databank and used as a template in the Prime module of Schrodinger suite. For homology model structure refinement, optimization of hydrogen bond assignments and minimization of side chain energies were done. Then, the generated homology model was validated and analyzed through Ramachandran plot in protein preparation wizard [28].

2.2. Active site prediction

The SiteMap tool in Maestro of Schrodinger Suite (v.12.8) was utilized in order to identify the active binding site regions in the homology model structure.

2.3. Ligand library preparation

The chemical structures of 3848 approved drugs were obtained from ChEMBL databases and prepared by ligPrep tool of Schrodinger Suite. The whole ligand optimization process was performed at pH 7.0. The 3D conformers were generated and Epik function was used to achieve the ionization state. Energy minimization was performed through the OPLS3e force field.

2.4. Docking of ChEMBL drugs

Glide Module was used for docking. Using Schrodinger's Standard Precision docking mode, the prepared drug library was docked against TMPRSS2. Extra Precision docking option was applied to the top drugs, and their protein-ligand complex interactions were assessed.

2.5. Molecular mechanics-generalized born and surface area (MM-GBSA)

Accurate binding free energy prediction of protein-ligand complexes was performed using Prime MM-GBSA. The refinement was conducted with the help of the VSGB continuum solvation model using water as a solvent.

2.6. Molecular dynamics (MD) simulation

Molecular dynamics (MD) simulations were performed for the top-five docking molecules to mimic physiological conditions using the Academic Desmond v6.5 by D.E. Shaw Research. The intent from that was to study the protein-ligand patterns of interaction and the conformational stability of complex systems. The temperature and pressure were set to be 300 k and 1.01325 bars, respectively, throughout the process for 50 ns and the OPLS3e force field was used in MD simulations.

2.7. Calculations of density functional theory

At last, density functional theory calculations were performed with the Jaguar module of Schrodinger. DFT calculations were used which allows employing a variety of functional to describe exchange and correlation for either open or closed-shell systems. B3LYP exchange correlation function was used beside the 6-31G** basis set. Standard Poisson-Boltzmann (PBF) was selected as solvation model using water as a solvent and maximum optimization steps were set to be 100 steps. In the self-consistent field (SCF), the level of accuracy, which adjusts the accuracy of pseudo-spectral calculations, was set to be quick. Finally, the molecular orbital, electron densities, electrostatic potential, and atomic electrostatic potential charges were calculated.

3. Results and discussion

3.1. Homology modeling

Since the TMPRSS2 crystal structure has not been solved yet, homology modeling was conducted as the first step. Human plasma kallikrein was used to build the model, which was then verified using the Ramachandran plot. TMPRSS2 model stereo chemical analysis displayed that about 99% of residues are in the favored region, which indicated that the model has good stereo chemical quality (Fig. 1).

3.2. Active site prediction

Using SiteMap tool, four sites were generated and the first site was selected owing to high site score of 1.016 and D score of 1.067 and additionally it contains the six amino acid residues Histidine 296, Aspartame 345, Serine 441, Aspartame 435, Serine 460, and Glycine 462 that are particularly essential in the active site of TMPRSS2 [21]. The amino acid residues that form the active site, including chain A: 296, 299, 300, 337, 340, 341, 342, 343, 345, 389, 418, 419, 420, 424, 435, 437, 438, 441, 460, 461, 462, 463, 464, 465, 473 and chain Z: 501 (Fig. 2).

3.3. Docking and MM-GBSA

From the 3848 approved drugs that were docked using SP mode of Glide, top 50 drugs with docking scores ≤ -7 were further docked using

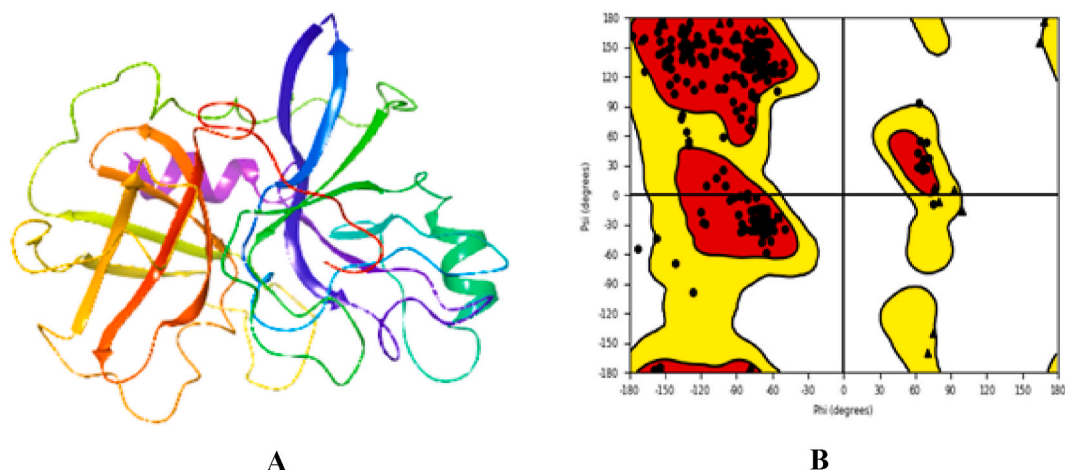


Fig. 1. Protein structures and Ramachandran plot. A. TMPRSS2 homology. B. Ramachandran plot.

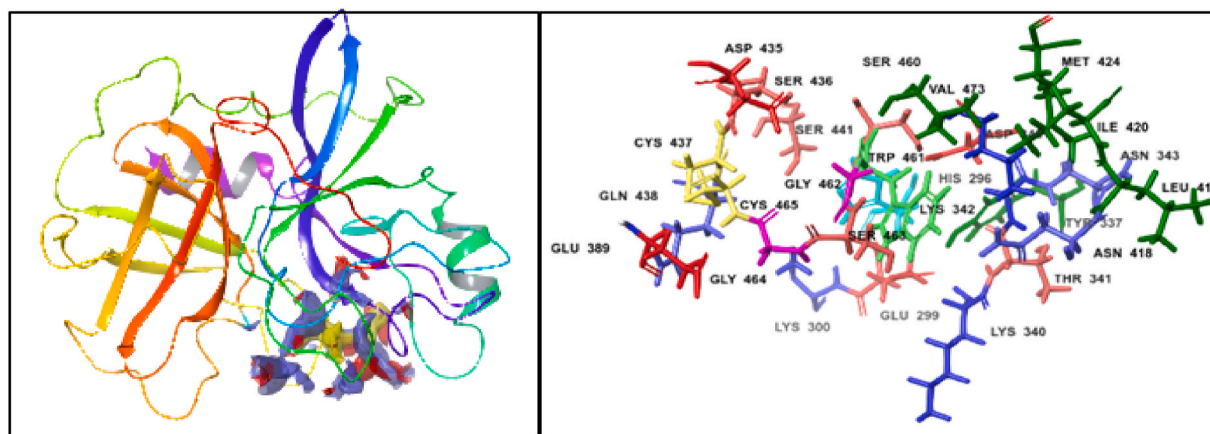


Fig. 2. Selected active site.

XP mode of Glide. The XP docking results were compared to the known two inhibitors of TMPRSS2 (ambroxol and nafamostat) as shown in Table 1.

The study revealed that 22 drugs have higher docking scores than the reference drugs. Among which, 18 drugs have MM-GBSA score higher than nafamostat and ambroxol.

Top five drugs with the highest docking scores among ChEMBL drugs; were amikacin, isepamicin, butikacin, lividomycin and paromomycin. Each drug has many types of interactions with the protein. For example amikacin, which has the highest docking score, has four types of interactions; pi-cation interaction with the LYS300, hydrogen bond interaction with GLU299, GLY464, ASP435, PO4501, salt bridges with ASP435, GLU299 and hydrophobic interaction with CYS437, TRP461, VAL473, CYS465, ALA466, PRO301 residues (Figs. 3 and 4).

All of the five drugs made interactions with one or more essential amino acid residues in TMPRSS2. Amikacin exhibited H-bond with GLY462 and salt bridge with ASP345. Isepamicin displayed H-bond with ASP345, ASP434 and SER441 and showed salt bridge with ASP435. Butikacin exhibited H-bond interaction with ASP345 and SER460 and salt bridge interaction with ASP345.while, lividomycin displayed pi-cation interaction with HIS296, H-bond with GLY462 and HIS296 and salt bridge with ASP345. Lastly, paromomycin showed hydrogen bond interaction with SER441, ASP345 and GLY462, and salt bridges with ASP345 and ASP435.

3.4. Molecular dynamics (MD) simulation

MD simulation study signifies structural understandings of the protein-ligand complex interaction based on the observed fluctuation in root mean square deviation (RMSD) and their capability to maintain their stability under simulated physiological circumstances, MD simulation was executed on the drugs that illustrated significant ligand-protein interactions, *i.e.*, amikacin, isepamicin, butikacin, lividomycin, and paromomycin, following XP-docking (Figs. 5-8).

The Amikacin-bound TMPRSS2 demonstrated hydrophilic and hydrophobic interactions during the molecular dynamic simulations. A diagram of C alpha structure formulated during the MD simulations was compared to the initial structures for RMSD analysis. During the 50 nsec of MD, the protein RMSD was clasped between 0.98 and 2.53 Å (Fig. 5). The residue CYS437 made full interaction with amikacin during the simulation. CYS437 and ASP440 formed H-bond with the ligand, which accounted for 99% and 98% respectively. Bridged H-bonds with several amino acid residues, *i.e.*, GLY439, ASP345, and HIS296 were observed during the simulation. Furthermore, HIS296 and TRP461 formed pi-cation bonds with the ligand, which accounted for 68% and 60% respectively as shown in Fig. 6.

Isepamicin-TMPRSS2 complex showed hydrophilic interactions during MD simulations. During the 50 nsec of MD, the protein RMSD remained between 0.92 and 2.37 Å to the end of the simulation. The ASP435 residue generated full interaction with the isepamicin, and SER436 was the second residue that made maximum contact with the

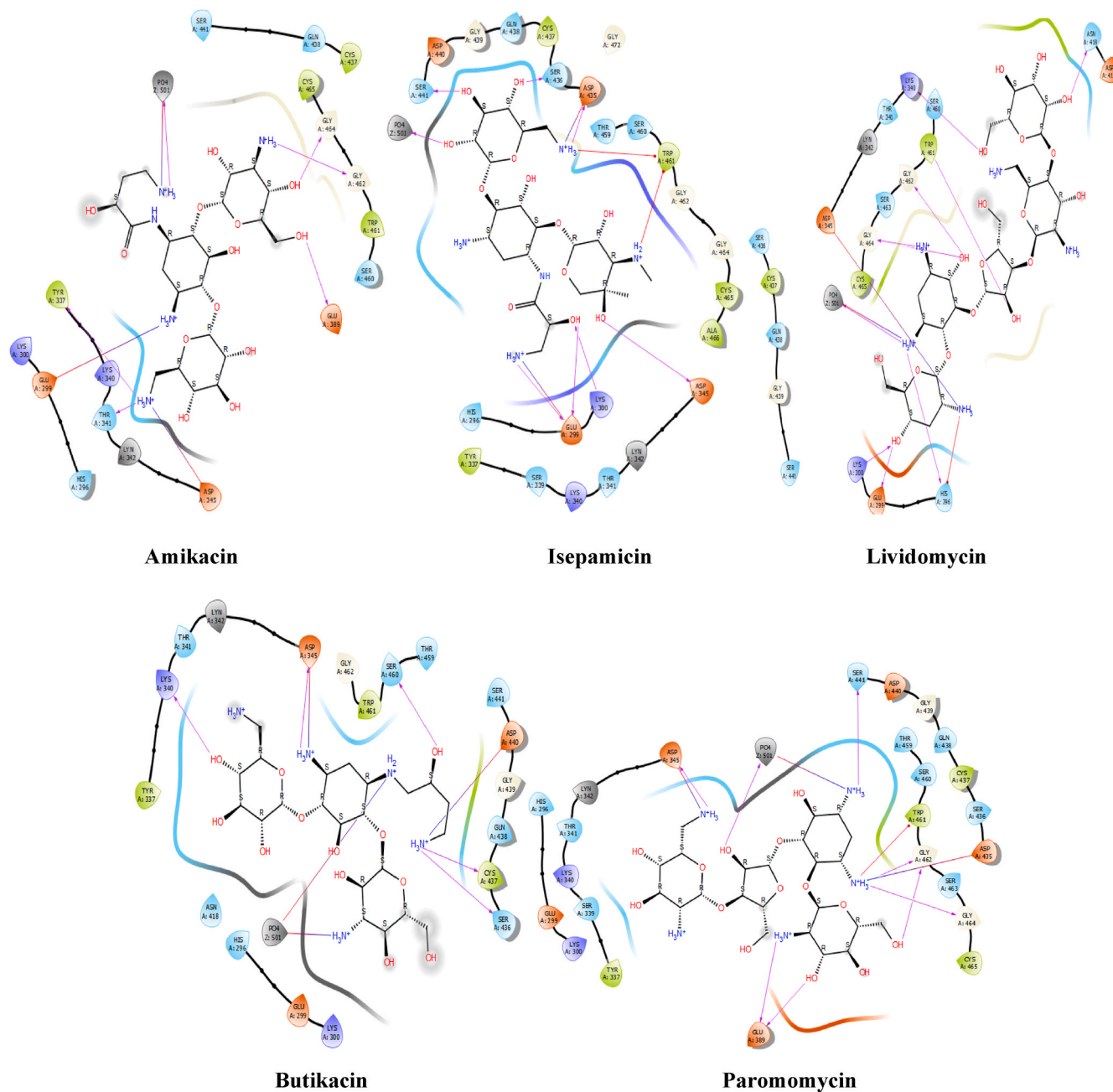


Fig. 3. 2D interactions of the top five drugs with TMPRSS2.

ligand. Hydrogen bonds were revealed with ASP435 and ASP345, which accounted for 98% and 91% of the interactions respectively. Moreover, the bridged H-bond with THR341 formed by 62% of the interactions was observed as displayed in Fig. 8. The butikacin-TMPRSS2 complex revealed hydrophobic and hydrophilic interactions during molecular dynamics simulations. Throughout the 50 nsec, the protein RMSD remained between 1.31 and 2.68 Å, until the end of the simulation. The ligand RMSD had an average of 1.5 Å, indicating a stable ligand-protein complex. The residues ASP345 and HIS296 showed ultimate contact with the ligand throughout simulations. Bridged H-bonds, pi-cation bonds, and direct H-bonds with protein residues were identified in the simulation. The amino acid HIS296 interacted with butikacin via a pi-cation, which persisted for 99% of the interaction. Bridged hydrogen bonds were observed between GLU299 and GLY464, which accounted for 79% and 60% respectively. Furthermore, ASP345, ASP440, and CYS437 make direct hydrogen bonds with the ligand, which accounted

for 99, 59, and 48% of the interaction respectively.

The lividomycin-bound TMPRSS2 illustrated hydrophilic and hydrophobic interactions during the MD simulations. During the 50 nsec of MD, and until the end of the MD simulation, the protein RMSD remained between 1.09 and 2.35 Å. The average of ligand RMSD was 1.7 Å, suggesting that the ligand is stable in the protein complex. The residue ASP417 and SER436 made the strongest bonds with lividomycin during the simulations. Bridged H-bonds with GLU389 and GLY462 were observed during the MD simulation. The amino acid residue HIS296 created pi-cation bond with the ligand, and SER436, GLU389, and GLY464, made direct hydrogen bonds which persisted for 97, 74, and 74% of the simulation time respectively, as represented in Fig. 8. TMPRSS2 protein bound with paromomycin complex showed hydrophilic interactions during molecular dynamics simulations. During the 50 nsec of MD, the protein RMSD was retained from 1.3 to 2.7 Å to the end of the simulation. The ligand RMSD has an average of 2.1 Å, which

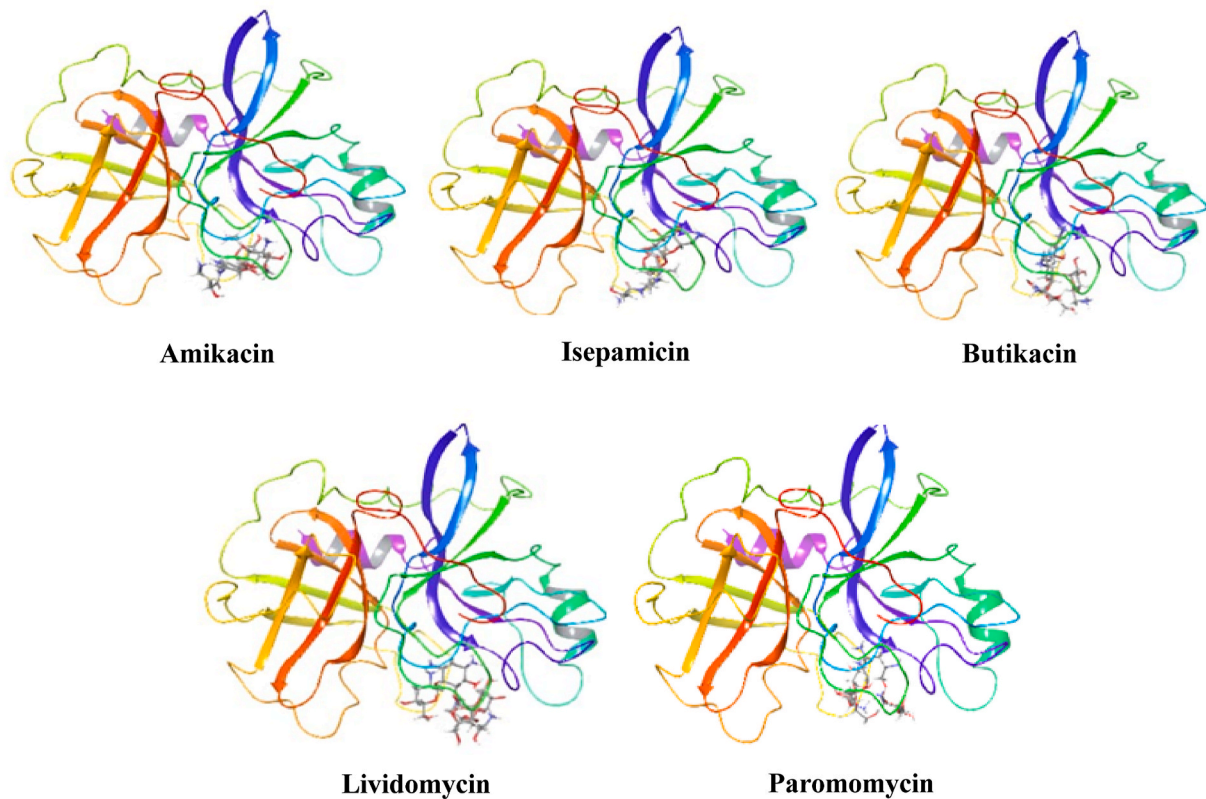


Fig. 4. 3D interactions of the top five drugs with TMPRSS2.

Table 1

docking score, MM-GBSA dG bind, and intermolecular interactions of references drugs (nafamostat and ambroxol) and XP high score ChEMBL drugs with TMPRSS2.

Name	Docking score	MM-GBSA dG bind	Pi-Pi interaction	Pi-cation interaction	Hydrogen bonding interaction	Salt bridges	Hydrophobic interaction
Nafamostat	-5.424	-59.76	-	LYS300	GLU299, GLY464, ASP435, PO4501	ASP435, GLU299	CYS437, TRP461, VAL473, CYS465, ALA466, PRO301
Ambroxol	-6.464	-55.48	-	HIS296	SER460, THR431	-	TYR337, TRP461, CYS437, CYS465
Amikacin	-14.919	-76.05	-	-	PO4501, GLY464, GLY462, GLU389, THR341, TYR337	PO451, GLU29, ASP345	TYR337, TRP461, CYS465, CYS437
Isepamicin	-14.750	-56.24	-	TRP461, TRP461	PO4 501, SER436, ASP435, SER441, ASP345, LYS300, GLU299, GLU299	GLU29, ASP435	TYR337, TRP461, CYS465, CYS437, ALA466
Butikacin	-13.307	-77.03	-	-	LYS340, ASP345, SER460, CYS437, SER436	PO450, PO451, ASP34, ASP440	TYR337, TRP461, CYS437
Lividomycin	-13.164	-68.40	-	HIS296	ASN418, LYS340, TRP461, GLY462, GLY464, PO4 501, LYS300, GLU299, HIS296	PO501, ASP345	TRP461, CYS465, CYS437
Paromomycin	-12.949	-85.29	-	-	PO4501, SER441, ASP345, GLY462, GLY464, GLY462, GLU389, GLU389	ASP345, ASP435	TYR337, TRP461, CYS465, CYS437
Arbekacin	-12.664	-65.98	-	TRP461, TRP461	ASP345, ASP435, GLU299	PO451, ASP435, GLU299	TYR337, TRP461, CYS465, CYS437, ALA466
Apramycin	12.316-	-79.31	-	-	ASP345, ASN418, THR341, SER460, SER436, GLY462	PO451, ASP435, ASP345, GLU299	TYR337, TRP461, CYS465, CYS437
Kanamycin	-11.641	-79.29	-	-	GLY462, PO4501, TYR337, GLU299, GLU389	PO451, ASP345	TYR337, TRP461, CYS465, CYS437
Butirosin	-11.535	-83.77	-	-	GLU299, GLU389, GLU389, THR341, THR341, TRP461	PO4 501, ASP345, GLU299	TYR337, TRP461, CYS465, CYS437
Bekanamycin	-11.344	-66.83	-	HIS296	ASN418, LYS340, LYS340, GLU299, LYS300, GLU299, GLU389	PO4 501, ASP345, ASP345, GLU299	TYR337, TRP461
Betamicin	10.685-	-67.93	-	TRP461, TRP461	SER460, THR341, LYS340, LYS340, ASN318, ASN318, ASP417	PO451, ASP345	TYR337, TRP461
Plazomicin	10.517-	-57.23	-	-	SER460, SER460, ASP345, THR341, GLU299, LYS300, PO4 501, PO4 501	PO451, ASP34, GLU299, GLU299	CYS437, CYS465, PRO301, VAL280, TYR337, TRP461
Propikacin	-10.331	-70.87	-	HIS296, TRP461, TRP461	ASN418, ASN418, LYN442, ASN418, ASN418, SER460	PO451, ASP345	TRP461, CYS437, LEU419

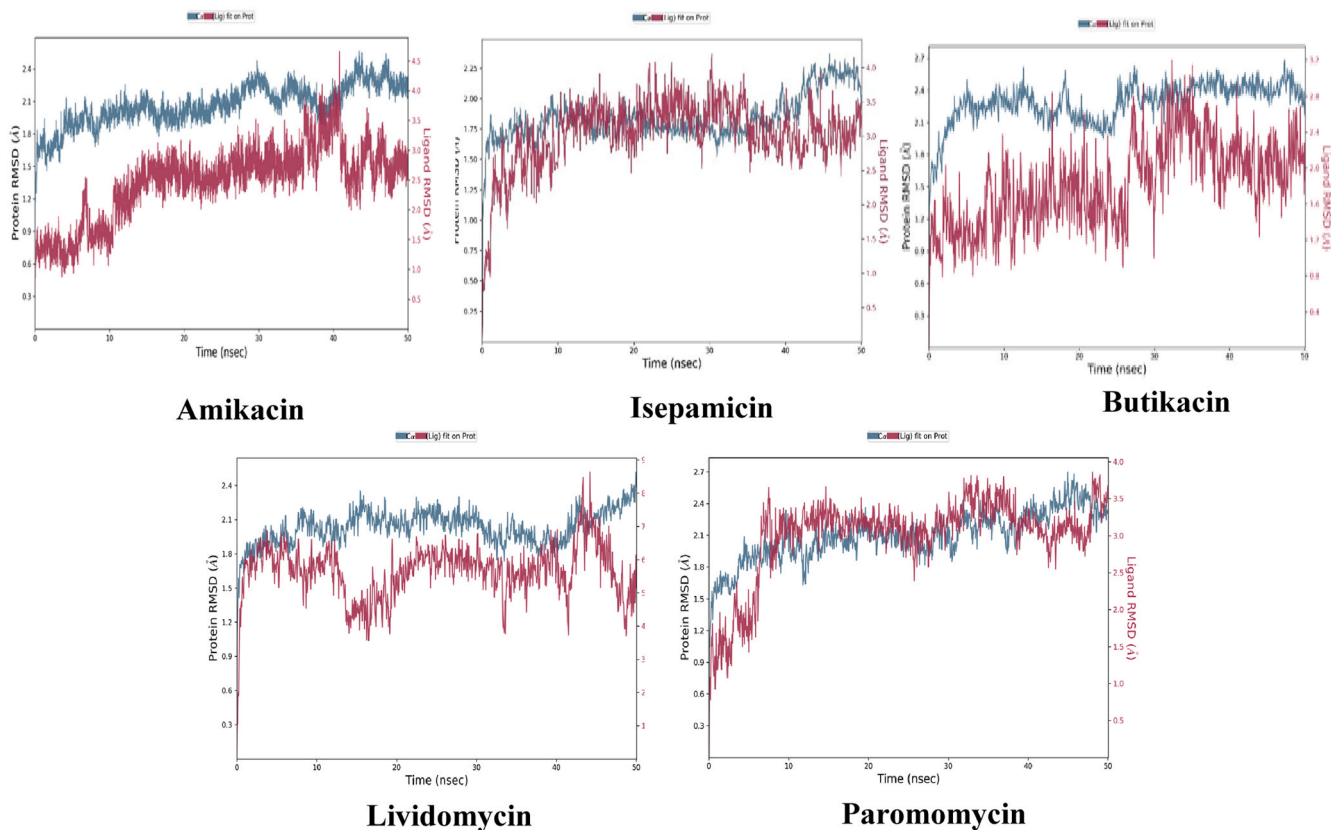


Fig. 5. Route mean square deviations (RMSD) plots.

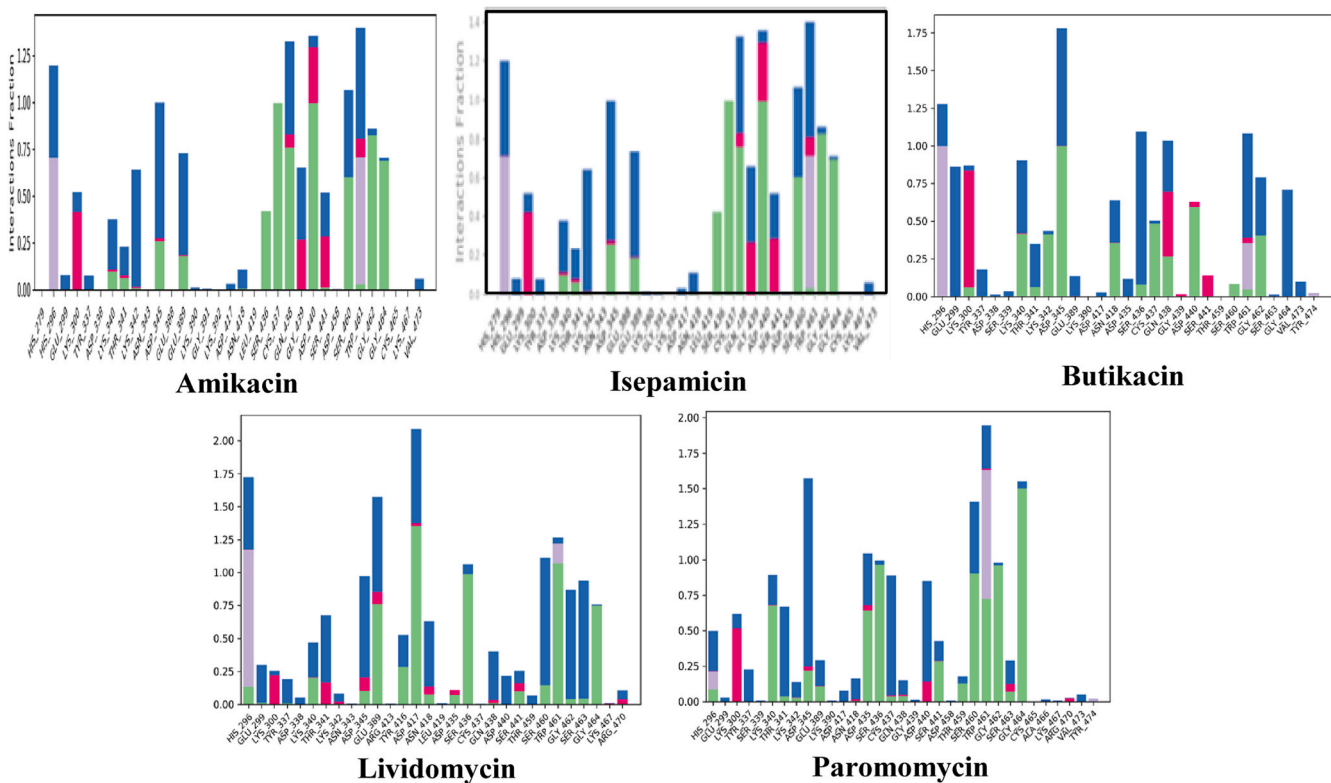


Fig. 6. The protein-ligand interaction diagram.

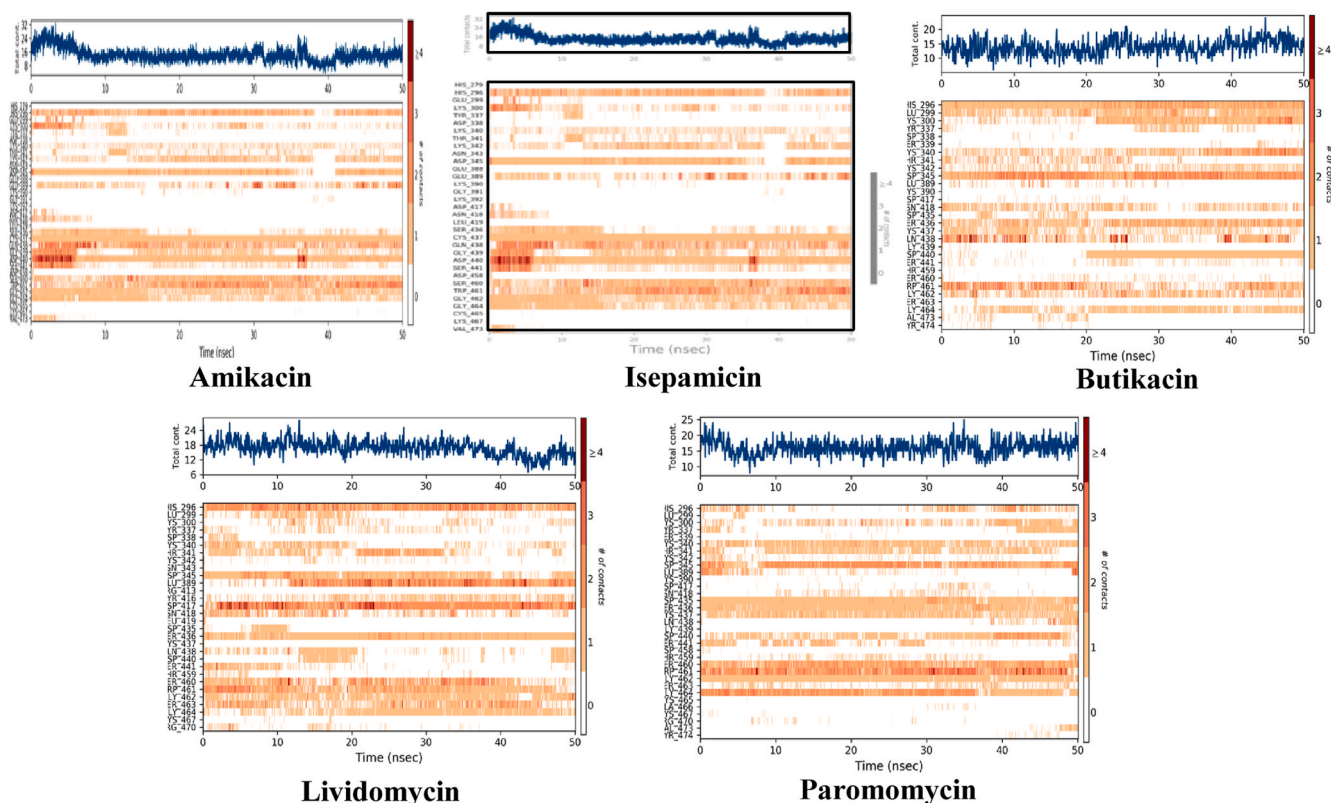


Fig. 7. Amino acid residues of protein that interact with the ligand.

suggested a highly stable ligand within the protein complex. GLY462 made ultimate interaction with the ligand during the simulation. In addition, bridged H-bond, and direct H-bond with protein's residues were identified. The amino acid GLY462 interacted with the drug via H-bonding, which accounted for 95% of the interactions. Other residues that formed H-bond with the drug are SER436, GLY462, and SER460, which persisted for 93%, 93%, and 84% of the simulation time respectively. Also bridged H-bonds with ASP345, THR341 formed by 61% and 58% for ASP345, and 47% for THR461 were observed.

These results suggest that paromomycin, amikacin, and isepamicin have the best binding among the shortlisted drugs.

3.5. DFT calculations

As shown in Table 2, the electronic properties of the top five drugs (amikacin, isepamicin, butikacin, lividomycin, and paromomycin) with good binding energies were determined. The five drug's HOMO and LUMO patterns (Figs. 9 and 10), energies, and energy differences were determined. For HOMO orbitals, a consistent negative value was observed. For examined drugs, the measured HOMO and LUMO range from -0.27 to 0.002 kcal/mol. HOMO and LUMO findings were both compared to the reference drugs nafamostat and ambroxol.

Butikacin has HOMO on O29 that interacts with LYS 340. Moreover, HOMO molecular orbitals are observed on O10, O34 and C32. The LUMO are found on N21, which interacts with PO4 501 and N27, which interacts with ASP 345. In addition, LUMO presents on C18, C19, C20, C30 and O12. The gap energy between the HOMO and LUMO was found to be -0.306 kcal/mol.

In paromomycin, HOMO orbitals are located on O14 and O29 that interact with the PO4 501. In addition, HOMO orbitals are found in O12, O13, O16, O42, C2, and C21. The LUMO orbitals are located on N32 which interacts with GLY 462, GLY 464, and ASP 435 as well as in C4, C24, O12 and O17. The energy gap between the HOMO and LUMO was found to be -0.277 kcal/mol.

Isepamicin, HOMO orbitals are located on O8, O9, O10, O23, O26, O27, O34, O35, O38, between C29 and C30, C30 and C31, C32 and C33, C3 and C4 and C4 and C5, all indicate the existence of possible reactive in these sites. While LUMO are located at O14, C12, C16 and N7. The energy gap between the HOMO and LUMO was found to be -0.265 kcal/mol.

Amikacin demonstrates that HOMO orbitals are found on O11, O13, C35, and C38 signifying the existence of possible reactive in the site. While LUMO orbitals are located on O11, C35, C38, H79, and N14. The energy gap between the HOMO and LUMO was found to be -0.261 kcal/mol.

In lividomycin, HOMO orbitals are located on O2, O15, O17, O24, O27, O29, C16 and C22. LUMO are located on N35 that interacts with TRP461 residue as well as on O31, O33, O37, O39, N41, C25, C34, C40 signifying the existence of possible reactive sites. The energy gap between the HOMO and LUMO was found to be -0.263 kcal/mol.

Molecular electrostatic potential MESP maps (Fig. 11) and their electrostatic potential energy, iso-potential profiles were generated for the top five drugs. Butikacin O26 interacts with LYS 340 shows the very strongly negative electrostatic potential susceptible to electrophiles (-146.29 kcal/mol). N21 interacts with PO4m501 and N27, which interacts with ASP345 that shows the very strongly positive electrostatic potential susceptible to nucleophiles (359.65 kcal/mol).

In paromomycin, O36 that interacts with the GLY 462 and O13 display a very strong negative electrostatic potential susceptible to electrophiles (-169.1265 kcal/mol). O15 and N28 that interacts with GLU 389 exhibit a strong positive electrostatic potential susceptible to nucleophiles (350.32 kcal/mol).

The most positive electrostatic potential in Isepamicin is related to N25 that interacts with ASP435 and TRP 461 (310.1312 kcal/mol), indicate their susceptibility to nucleophiles. While the most negative electrostatic potential is related to O34, O38, O27, which interacts with SER 441, indicate their susceptibility to electrophiles.

Regarding amikacin, the most positive electrostatic potential is

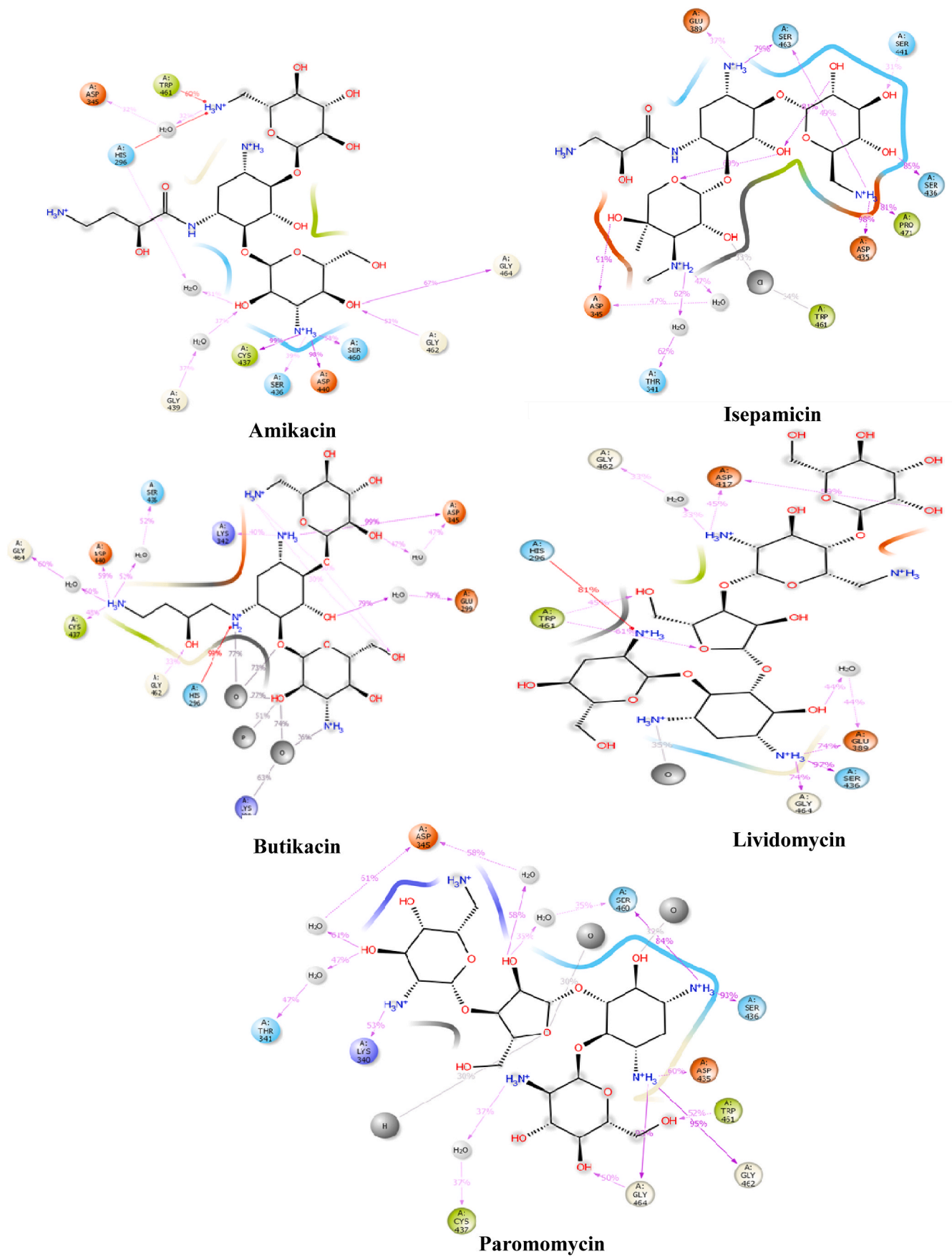


Fig. 8. PL-contacts diagram.

Table 2
Quantum chemical proprieties of the references and top five drugs.

Drug	HOMO (kcal/mol)	LUMO (kcal/mol)	HLG (kcal/mol)	Solvation Energy (kcal/mol)
Ambroxol (control)	-0.22955	-0.04444	-0.185	-55.25
Nafamostat (control)	-0.23571	-0.07482	-0.160	-148.16
Butikacin	-0.27522	0.03120	-0.306	-726.72
Paromomycin	-0.26664	0.01076	-0.277	-690.03
Isepamicin	-0.269616	-0.00415	-0.265	-463.65
Amikacin	-0.25864	0.00228	-0.261	-494.64
Lividomycin	-0.25900	0.00351	-0.263	-682.23

related to H42, N16 that interacts with GLY 462, N15 that interacts with GLU 299 (288.08 kcal/mol), indicate their susceptibility to nucleophiles. Whereas the most negative electrostatic potential is related to O7, O8, and O10 which interacts with GLY 461, O12 that interacts with GLU 389 (121.53 kcal/mol), indicate their susceptibility to electrophiles.

In lividomycin, O48 that interacts with ASP 417, O49 and O50 display strong negative electrostatic potential to electrophiles (80.86 kcal/mol). While, N20, N35 and N41 show a strong positive electrostatic potential susceptible to nucleophiles (352.1 kcal/mol). Nitrogen 35 interacts with ASP417 and GLY462.

4. Discussion

The lack of adequate knowledge about COVID-19 pathophysiology, as well as a well-defined treatment strategy or a possible medication to treat SARS-CoV-2 infection, has caused the recently emerging life-threatening viral disease to spread at an alarming pace [29]. Repurposing known drugs tend to be a very powerful way to immediately develop effective coronavirus drugs in a short period. The protease TMPRSS2 cleaves the SARS-CoV-2 spike protein, allowing the virus to

enter and activate. Given the difficulty in obtaining the crystal structure of TMPRSS2 and the lack of structural details, computational modeling and molecular docking represents feasible, efficient, and cost-effective techniques for identifying potential TMPRSS2 inhibitors.

The docking analysis of 3848 drugs from the ChEMBL database and further MM-GBSA, MD and DFT studies revealed that amikacin, isepamicin, butikacin, lividomycin, and paromomycin have high binding energy and stable interactions with TMPRSS2 in current computational research. Aminoglycosides could be used as a scaffold to develop COVID-19 medicinal compounds, but *in vitro* and *in vivo* research is needed before using them as an anti-COVID-19 drug [30]. The activity of aminoglycosides against SARS-CoV-2 may be owing to the formation of retrocyclins, a bioactive peptide obtained from human theta-defensins that blocks SARS-CoV-2 cellular fusion and aggregation [31].

Amikacin is a kanamycin-derived semisynthetic aminoglycoside antibiotic with activity against the resistant gram-negative bacteria and *Pseudomonas aeruginosa* [32]. Amikacin is the most effective second-line injectable anti-tuberculosis drug and still encouraged for multi-drug-resistant tuberculosis. It is only considered for a short MDR-TB regimen [33].

Isepamicin is one of the most effective drugs against both mycobacterium intracellular and mycobacterium avium isolates and can serve as an alternative aminoglycoside if toxicity or unfavorable consequences are main concerns as it has much less nephro-, vestibulo-, ototoxicity than other aminoglycosides [34]. In the case of isepamicin no individual adverse event was reported in more than 2% of patients, the most commonly reported events are phlebitis, rash, headaches and renal compromise [35].

Butikacin is an aminoglycoside antibiotic that has the cochlear toxicity profile of kanamycin A [36]. Lividomycin is an aminoglycoside composed mainly of paromomycin and lividomycin B [37]. Paromomycin was proven to be effective in the treatment of asymptomatic and mild symptomatic amoebiasis, with few side effects, including diarrhea, nausea, headache and dizziness [38].

Amikacin and paramomycin were considered as the most effective

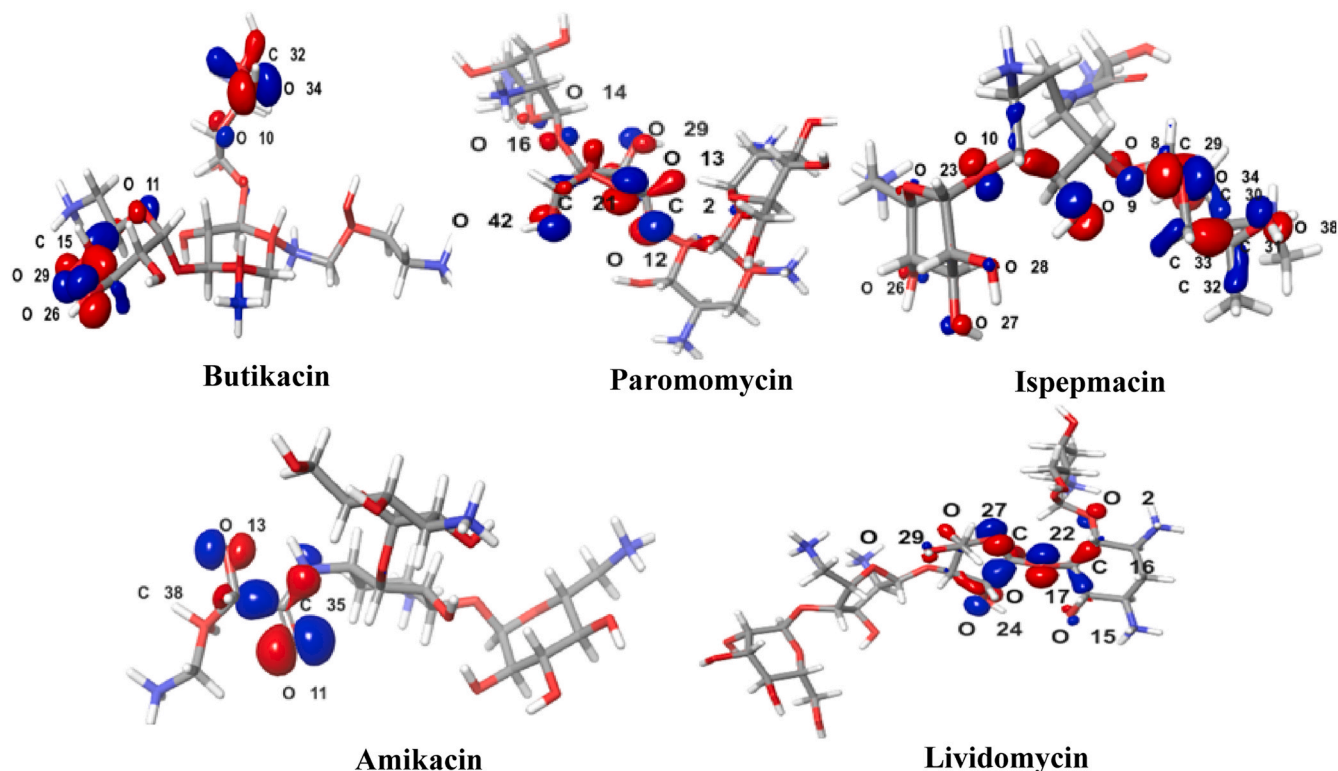


Fig. 9. HOMO representation of top five drugs.

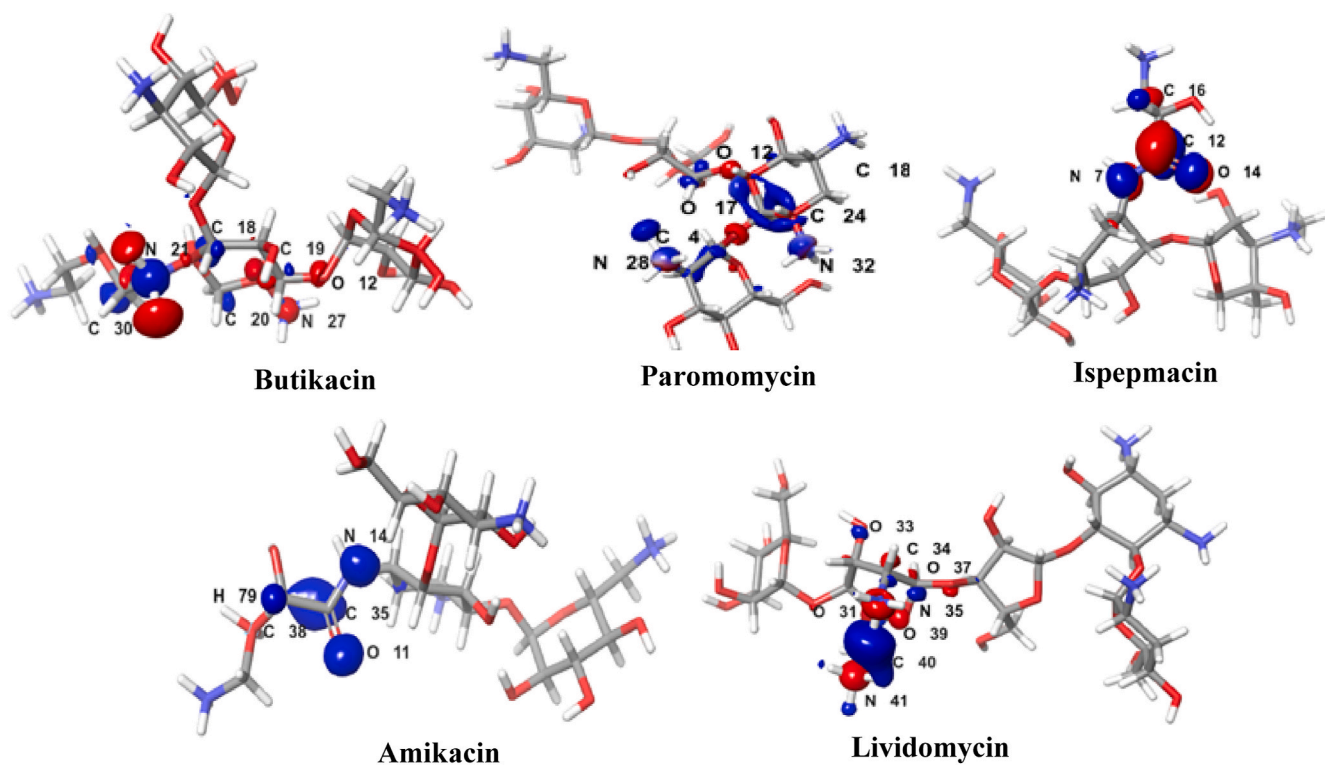


Fig. 10. LUMO representation of top five drugs.

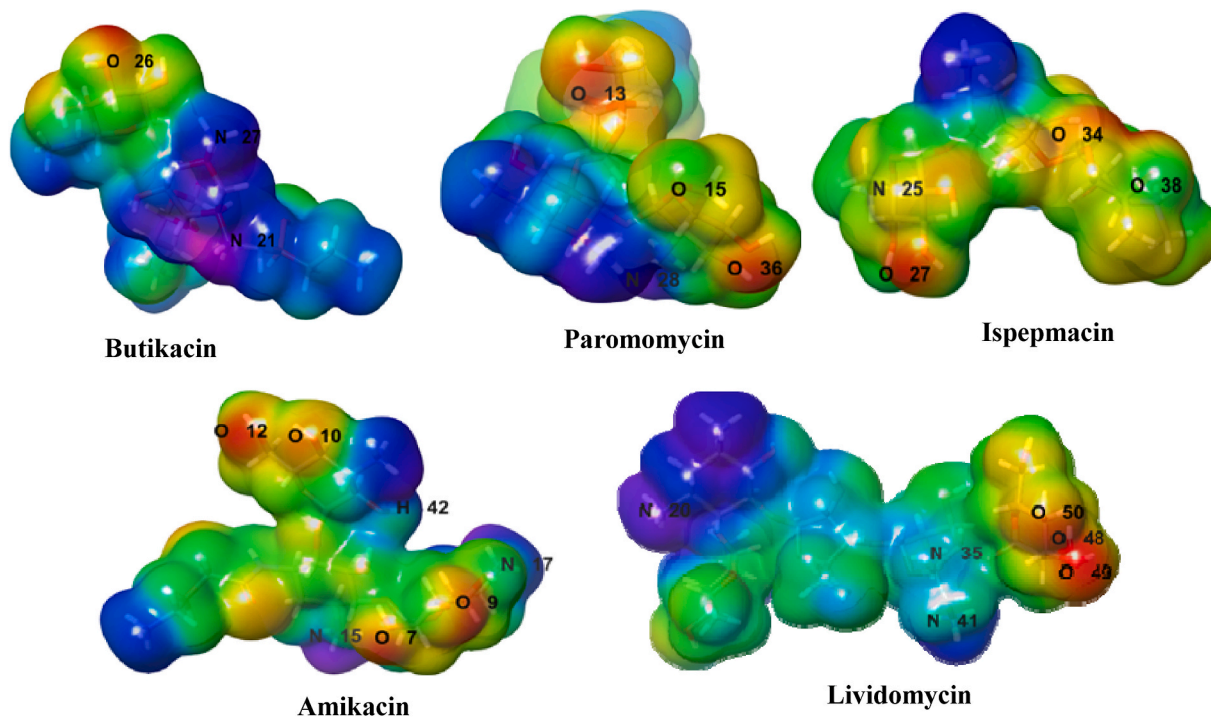


Fig. 11. Electrostatic representation of top five.

drug candidates showing the highest binding affinity against another SARS-CoV-2 protein (Mpro) [30]. According to another *in silico* experiment, lividomycin is an effective therapeutic candidate for inhibiting ACE2, therefore impairing one of the key proteins identified by SARS-CoV-2 for cell entry [39]. Also Paromomycin has been considered as a therapeutic target for COVID-19 management due to its high binding affinity for the RDB protein [40].

5. Conclusion

The TMPRSS2 enzyme has been considered a key target for COVID-19 infection suppression. In this research, the structure-based virtual screening addressed five commercially available drugs amikacin, ispepmacin, butikacin, lividomycin, and paromomycin, which could inhibit the TMPRSS2 enzyme. These drugs have known efficacy and ADMET

properties and thus might be repurposed for COVID-19 treatment.

Declaration of competing interest

The authors declare that they have no known competing financial interests or personal relationships that could have appeared to influence the work reported in this paper.

Acknowledgment

We acknowledge Mme Katia Dekimeche from Schrodinger for her support and help.

References

- Englich CN, Tschernig T, Flockerzi F, Meier C, Bohle RM. Lesions in the lungs of fatal corona virus disease Covid-19. *Ann Anat* 2021;234:151657. <https://doi.org/10.1016/j.aanat.2020.151657>.
- Xiao T, Wei Y, Cui M, Li X, Ruan H, Zhang L, Bao J, Ren S, Gao D, Wang M, Sun R, Li M, Lin J, Li D, Yang C, Zhou H. Effect of dihydromyricetin on SARS-CoV-2 viral replication and pulmonary inflammation and fibrosis. *Phytomedicine* 2021;91:153704. <https://doi.org/10.1016/j.phymed.2021.153704>.
- WHO coronavirus (COVID-19) dashboard | WHO coronavirus (COVID-19) dashboard with vaccination data. 2021 (accessed June 15, 2021), <https://covid19.who.int/>.
- Li C, Yang Y, Ren L. Genetic evolution analysis of 2019 novel coronavirus and coronavirus from other species. *Infect Genet Evol* 2020;82:1–3. <https://doi.org/10.1016/j.meegid.2020.104285>.
- Su S, Wong G, Shi W, Liu J, Lai ACK, Zhou J, Liu W, Bi Y, Gao GF. Epidemiology, genetic recombination, and pathogenesis of coronaviruses. *Trends Microbiol* 2016;24:490–502. <https://doi.org/10.1016/j.tim.2016.03.003>.
- Zhu N, Zhang D, Wang W, Li X, Yang B, Song J, Zhao X, Huang B, Shi W, Lu R, Niu P, Zhan F, Ma X, Wang D, Xu W, Wu G, Gao GF, Tan W. A novel coronavirus from patients with pneumonia in China, 2019. *N Engl J Med* 2020;382:727–33. <https://doi.org/10.1056/nejmoa2001017>.
- Glowacka I, Bertram S, Muller MA, Allen P, Soilleux E, Pfefferle S, Steffen I, Tsegaye TS, He Y, Gnirss K, Niemeyer D, Schneider H, Drosten C, Pohlmann S. Evidence that TMPRSS2 activates the severe acute respiratory syndrome coronavirus spike protein for membrane fusion and reduces viral control by the humoral immune response. *J Virol* 2011;85:4122–34. <https://doi.org/10.1128/jvi.02232-10>.
- Hoffmann M, Kleine-Weber H, Schroeder S, Krüger N, Herrler T, Erichsen S, Schiergens TS, Herrler G, Wu NH, Nitsche A, Müller MA, Drosten C, Pöhlmann S. SARS-CoV-2 cell entry depends on ACE2 and TMPRSS2 and is blocked by a clinically proven protease inhibitor. *Cell* 2020;181:271–80. <https://doi.org/10.1016/j.cell.2020.02.052>.
- Ragia G, Manolopoulos VG. Inhibition of SARS-CoV-2 entry through the ACE2/TMPRSS2 pathway: a promising approach for uncovering early COVID-19 drug therapies. *Eur J Clin Pharmacol* 2020;76:1623–30. <https://doi.org/10.1007/s00228-020-02963-4>.
- V'kovski P, Kratzel A, Steiner S, Stalder H, Thiel V. Coronavirus biology and replication: implications for SARS-CoV-2. *Nat Rev Microbiol* 2021;19:155–70. <https://doi.org/10.1038/s41579-020-00468-6>.
- Zhou Y, Vedantham P, Lu K, Agudelo J, Carrion R, Nunneley JW, Barnard D, Pöhlmann S, McKerrow JH, Renslo AR, Simmons G. Protease inhibitors targeting coronavirus and filovirus entry. *Antivir Res* 2015;116:76–84. <https://doi.org/10.1016/j.antiviral.2015.01.011>.
- Gierer S, Bertram S, Kaup F, Wrensch F, Heurich A, Kramer-Kuhl A, Welsch K, Winkler M, Meyer B, Drosten C, Dittmer U, von Hahn T, Simmons G, Hofmann H, Pöhlmann S. The spike protein of the emerging betacoronavirus EMC uses a novel coronavirus receptor for entry, can be activated by TMPRSS2, and is targeted by neutralizing antibodies. *J Virol* 2013;87:5502–11. <https://doi.org/10.1128/jvi.00128-13>.
- Heurich A, Hofmann-winkler H, Gierer S, Liepold T, Jahn O. Proteolysis by TMPRSS2 augments entry driven by the severe. *Acute* 2014;88:1293–307. <https://doi.org/10.1128/JVI.02202-13>.
- Matsuyama S, Nao N, Shirato K, Kawase M, Saito S, Takayama I. Enhanced isolation of SARS-CoV-2 by TMPRSS2-expressing cells. 2020. p. 1–3. <https://doi.org/10.1073/pnas.2002589117>.
- Iwata-yoshikawa N, Okamura T, Shimizu Y, Hasegawa H, Takeda M, Nagata N, Health G. TMPRSS2 contributes to virus spread and immunopathology in the airways of murine models after coronavirus infection. 2019. <https://doi.org/10.1128/JVI.01815-18>.
- Singh R, Kumar V, Das P, Purohit R. A computational approach for rational discovery of inhibitors for non-structural protein 1 of SARS-CoV-2. *Comput Biol Med* 2021;135:104555. <https://doi.org/10.1016/j.combiomed.2021.104555>.
- Shen LW, Mao HJ, Wu YL, Tanaka Y, Zhang W. TMPRSS2: a potential target for treatment of influenza virus and coronavirus infections. *Biochimie* 2017;142:1–10. <https://doi.org/10.1016/j.biochi.2017.07.016>.
- Vk B, R S, P D, R P. Evaluation of acridinedione analogs as potential SARS-CoV-2 main protease inhibitors and their comparison with repurposed anti-viral drugs. *Comput Biol Med* 2021;128. <https://doi.org/10.1016/j.COMPBIO.2020.104117>.
- R S, Vk B, J S, R P, S K. In-silico evaluation of bioactive compounds from tea as potential SARS-CoV-2 nonstructural protein 16 inhibitors. *J. Tradit. Complement. Med* 2021. <https://doi.org/10.1016/J.JTCME.2021.05.005>.
- J S, V KB, R S, V R, R P, S K. An in-silico evaluation of different bioactive molecules of tea for their inhibition potency against non structural protein-15 of SARS-CoV-2. *Food Chem* 2021;346. <https://doi.org/10.1016/J.FOODCHEM.2020.128933>.
- Idris MO, Yekeen AA, Alakanse OS, Durojaye OA. Computer-aided screening for potential TMPRSS2 inhibitors: a combination of pharmacophore modeling, molecular docking and molecular dynamics simulation approaches. *J Biomol Struct Dyn* 2020:1–19. <https://doi.org/10.1080/07391102.2020.1792346>.
- Basu S, Veerarahavan B, Ramaiah S, Anbarasu A. Novel cyclohexanone compound as a potential ligand against SARS-CoV-2 main-protease. *Microb Pathog* 2020;149:104546. <https://doi.org/10.1016/j.micpath.2020.104546>.
- Broggi S, Ramalho TC, Kuca K, Medina-Franco JL, Valko M. Editorial: in silico methods for drug design and discovery. *Front. Chem.* 2020:612. <https://doi.org/10.3389/FCHEM.2020.00612>.
- Anbarasu A, Ramaiah S, Livingstone P. Vaccine repurposing approach for preventing COVID 19: can MMR vaccines reduce morbidity and mortality? *Hum Vaccines Immunother* 2020;16:2217–8. <https://doi.org/10.1080/21645515.2020.1773141>.
- Durdagi S. Virtual drug repurposing study against SARS-CoV-2 TMPRSS2 target. *Turkish J Biol* 2020;44:185–91. <https://doi.org/10.3906/biy-2005-112>.
- Zaki AM, van Boheemen S, Bestebroer TM, Osterhaus ADME, Fouchier RAM. Isolation of a novel coronavirus from a man with pneumonia in Saudi Arabia. *N Engl J Med* 2012;367:1814–20. <https://doi.org/10.1056/nejmoa1211721>.
- Li Z, Partridge J, Silva-Garcia A, Rademacher P, Betz A, Xu Q, Sham H, Hu Y, Shan Y, Liu B, Zhang Y, Shi H, Xu Q, Ma X, Zhang L. Structure-guided design of novel, potent, and selective macrocyclic plasma kallikrein inhibitors. *ACS Med Chem Lett* 2017;8:185–90. <https://doi.org/10.1021/acsmchemlett.6b00384>.
- Hollingsworth SA, Karplus PA. A fresh look at the Ramachandran plot and the occurrence of standard structures in proteins. *Biomol Concepts* 2010;1:271–83. <https://doi.org/10.1515/BMC.2010.022>.
- Zheng J. SARS-coV-2: an emerging coronavirus that causes a global threat. *Int J Biol Sci* 2020;16:1678–85. <https://doi.org/10.7150/ijbs.45053>.
- Ahmed MZ, Zia Q, Haque A, Alqahtani AS, Almarfadi OM, Banawas S, Alqahtani MS, Ameta KL, Haque S. Aminoglycosides as potential inhibitors of SARS-CoV-2 main protease: an in silico drug repurposing study on FDA-approved antiviral and anti-infection agents. *J. Infect. Public Health.* 2021;14:611–9. <https://doi.org/10.1016/j.jiph.2021.01.016>.
- Chalichem NSS, Bethapudi B, Mundkinajeddu D. Aminoglycosides can be a better choice over macrolides in COVID-19 regimen: plausible mechanism for repurposing strategy. *Med Hypotheses* 2020;144:109984. <https://doi.org/10.1016/j.mehy.2020.109984>.
- O. Sizar, S. Rahman, V. Sundareshan, COVID-19 information amikacin contraindications continuing education 2021 [online], available at: <https://www.ncbi.nlm.nih.gov/books/NBK430908/> [accessed 20 March 2021].
- Islam M, Tan Y, Hameed HMA, Liu Y, Chhotaray C, Cai X, Liu Z, Lu Z, Wang S. Journal of Global Antimicrobial Resistance Prevalence and molecular characterization of amikacin resistance among Mycobacterium tuberculosis clinical isolates from southern China. *Integr. Med. Res.* 2020;22:290–5. <https://doi.org/10.1016/j.jgar.2020.02.019>.
- Huang C, Wu M, Chen H. ScienceDirect in vitro activity of aminoglycosides, clofazimine, D-cycloserine and dapson against 83 Mycobacterium avium complex clinical isolates. *J Microbiol Immunol Infect* 2017;1–8. <https://doi.org/10.1016/j.jmii.2017.05.001>.
- Levéque D, Becker G, Bilger K, Natarajan-Amé S. Clinical pharmacokinetics and pharmacodynamics of dasatinib. *Clin Pharmacokinet* 2020;59:849–56. <https://doi.org/10.1007/s40262-020-00872-4>.
- Carter AJ. Cochlear toxicity of butikacin (UK-18,892), a new semisynthetic aminoglycoside antibiotic, in Guinea pigs. *Antimicrob Agents Chemother* 1979;16:362–5. <https://doi.org/10.1128/AAC.16.3.362>.
- Oda T, Mori T, Itô H, Kunieda T, Munakata K. Studies on new antibiotic lividomycins. I. Taxonomical studies on the lividomygin-producing strain streptomyces lividus nov. SP. *J Antibiot (Tokyo)* 1971;24:333–8. <https://doi.org/10.7164/antibiotics.24.333>.
- Kikuchi T, Koga M, Shimizu S, Miura T, Maruyama H, Kimura M. Parasitology International Efficacy and safety of paromomycin for treating amebiasis in Japan. *Parasitol Int* 2013;62:497–501. <https://doi.org/10.1016/j.parint.2013.07.004>.
- Terali K, Baddal B, Gülcan HO. Prioritizing potential ACE2 inhibitors in the COVID-19 pandemic: insights from a molecular mechanics-assisted structure-based virtual screening experiment. *J Mol Graph Model* 2020;100. <https://doi.org/10.1016/j.jmgm.2020.107697>.
- Tariq A, Mateen RM, Afzal MS, Saleem M. Paromomycin: a potential dual targeted drug effectively inhibits both spike (S1) and main protease of COVID-19. *Int J Infect Dis* 2020;98:166–75. <https://doi.org/10.1016/j.ijid.2020.06.063>.